Au Atoms and Dimers on the MgO(100) Surface: A DFT Study of Nucleation at Defects

Annalisa Del Vitto and Gianfranco Pacchioni*

Dipartimento di Scienza dei Materiali, Università Milano-Bicocca, via R. Cozzi 53, I-20125 Milano, Italy

Françoise Delbecq and Philippe Sautet

Laboratoire de Chimie, UMR 5182, CNRS, Ecole Normale Superieure de Lyon, 46 Allee d'Italie, 69364 Lyon Cedex 07, France

Received: December 23, 2004; In Final Form: February 14, 2005

The adsorption of Au atoms at the surface of MgO and the formation of Au dimers have been studied by means of first principles DFT supercell calculations. Au atoms have been adsorbed on flat MgO terraces and monatomic steps but also at point defects such as oxygen vacancies (F centers) or divacancies. Very low barriers for diffusion of Au atoms on the MgO(100) terraces have been found. Atom diffusion is stopped only at strong binding sites such as the F and F^+ centers (adsorption energy $E_a = 3-4$ eV), divacancies ($E_a = 2.3$ eV), or, to less extent, steps ($E_a = 1.3$ eV). The combination of two Au adatoms with formation of a dimer is accompanied by an energy gain, the dimer binding energy, E_b, between 2 and 2.4 eV for all sites considered, with the exception of the paramagnetic F^+ center where the gain is negligible (0.3 eV). The dimerization energy on the surface is not too different from the bond strength of Au_2 in the gas phase (2.32 eV). Thus, defects sites on MgO do not have a special role in promoting or demoting Au dimerization, while they are essential to trap the diffusing Au atoms or clusters. Calculations on Au_3 formed on an F center show that the cluster is fluxional.

1. Introduction

Size-selected metal atoms and clusters on oxide surfaces represent well-defined models of complex heterogeneous catalysts.[1−3] The properties of the deposited nanoclusters depend on the cluster size, but also on the oxide substrate and in particular on the presence of point and extended defects where the cluster is stabilized.[4−6] Therefore, a detailed characterization of the sites where metal particles are bound at the surface of oxide single crystals or thin films is essential to identify the structure−property relationships. Pd and Au atoms and clusters deposited on MgO thin films or single crystals have been studied both theoretically and experimentally.[1−8] Point defects at the surface of MgO play an important role not only in trapping the metal atoms and in facilitating the cluster growth, but also in promoting the catalytic activity of the supported clusters.[4,5] This has stimulated a specific activity aimed at the identification of the point defects involved in the nucleation and growth of metal nanoclusters.[9,10]

The number of potential candidates as trapping sites at the surface of MgO is quite large,[11] and a careful comparison of experimental measurements and computational simulations can provide important insight into the problem. Recently, it has been shown that the properties of CO molecules adsorbed on MgO-supported Pd atoms can be very useful to identify the surface sites where the atoms are bound.[12−14] Theory has proved very helpful also to gain insight into the mechanisms of the deposition and nucleation of metal atoms and clusters. Under typical growth conditions, dimers constitute the first step in island nucleation. Recent atomic force microscopy (AFM) measurements on the growth of Pd clusters on MgO(100) have shown defect-controlled nucleation. There is a general consensus that oxygen vacancies at the surface of MgO, characterized by the presence of one or two electrons trapped in the cavity (F^+ and F centers, respectively), act as strong traps for the metal atoms diffusing on the surface.[4,10] However, according to recent first principle calculations the most widely studied point defect in MgO, the F center, is inefficient for nucleation of late transition metals,[15] leaving open the question of the sites where metal clusters nucleate.

Many theoretical and experimental studies have addressed the deposition and growth of Au clusters on MgO.[5,20−23] So far, however, a systematic study of the adsorption of Au atoms on various MgO sites, and on the formation of Au_2 from the diffusion of isolated atoms, is still lacking. Our aim in this study was to analyze in detail the nucleation mechanisms determining the metal growth on the MgO surface. We have performed density functional theory (DFT) calculations, and we have considered adsorption and dimerization on terrace sites, oxygen vacancies (both neutral and charged +1), monatomic steps, and divacancies. The study parallels a similar one on the dimerization of Pd on the same sites of MgO. While Pd has a closed shell atomic state, ^1S ($4d^{10}$), Au has a ^2S ($5d^{10}6s^1$) configuration; clearly, the interaction with defects such as an F center could be different for the two metals, and a comparison of the two atoms can help to establish some general rules.

The paper is organized as follows. In section 2 we give the main details of the calculations and of the models used. Section 3 reports the results for Au atoms and dimers; we discuss not only the energetic aspects of the interaction but also the bond nature, the occurrence of charge transfers, and the position of metal-induced states in the gap. Preliminary results on the structure of a Au_3 cluster formed on an oxygen vacancy are

* To whom correspondence should be addressed. E-mail: Gianfranco.pacchioni@mater.unimib.it.

10.1021/jp044143+ CCC: $30.25
Published on Web 03/26/2005

TABLE 1. Properties of Au Atoms and Dimers Adsorbed at Regular and Defect Centers of the MgO Surface

	O_{5c}, terrace	O_{4c}, step	F_s center	F_s^+ center	divacancy
		Monomer			
E_a,[a] eV	0.89	1.26	3.17	3.97	2.34
r(Au−S), Å	2.28	2.20	2.82	2.79	2.44
z(Au−S), Å	2.28		1.79	1.56	0.48
		Dimer			
E_a,[a] eV	1.49	2.07	4.17	2.82	2.97
E_{dim},[b] eV	2.91	3.12	3.21	1.17	2.95
E_b,[c] eV	1.99	2.23	2.42	0.26	2.06
r(Au−S), Å	2.18	2.10	2.71	2.84	2.31
r(Au−Au), Å	2.53	2.55	2.73	2.64	2.71

[a] $E_a = -E(Au_n/MgO\ site) + E(Au_n) + E(MgO\ site)$, $n = 1$ or 2. [b] $E_{dim} = -E(Au_2/MgO\ site) + E(Au) + E(Au_1/MgO\ site)$. [c] $E_b = -E(Au_2/MgO\ site) - E(MgO\ O_{5c}) + E(Au_1/MgO\ site) + E(Au_1/MgO\ O_{5c})$.

also presented. Some general conclusions and a discussion of the growth mode of Au clusters on MgO are given in the last section.

2. Computational Details

The calculations are based on gradient-corrected DFT,[24,25] using the Vienna ab initio simulation program (VASP).[26] The program solves the Kohn−Sham equations of the density functional theory with the expansion of the one-electron wave functions in a plane waves basis set. The electron−ion interactions are described by the projector-augmented wave method (PAW) developed by Blöchl.[27] This is basically an all-electron frozen core method combining the accuracy of all-electron methods with the computational simplicity of the pseudopotential approach. The 2p orbitals of Mg have been included in the valence. In this framework, a tight convergence of the plane wave expansion was obtained with a kinetic energy cutoff of 265.6 eV. The generalized gradient approximation (GGA) has been chosen to represent the exchange-correlation potential in the formulation of Perdew and Wang (PW-91).[28] The MgO(100) surface has been modeled for the terrace by a three-layer slab. Theoretical calculations and electronic structure measurements on ultrathin MgO films have shown that the properties are well converged for three-layer films.[29] Besides, we have performed some calculations to test the effect of the slab thickness on the energy data. Going from three to four MgO layers, the binding energies change at most by 0.01 eV, a sign of a convergence of the results versus slab thickness. Supercells (4×4) containing 96 atoms each have been used for the terrace, while for the step we have employed the (310) surface, with a three-layer super cell containing 22 O and 22 Mg atoms. Convergence versus supercell size has been checked by considering in selected cases 5×5 supercells for the terrace and the (510) surface for the step. Since the general features do not change, the calculations have been performed with the smaller cells. The upper two layers are relaxed, while the atoms in the third layer are frozen in their lattice positions (Mg−O distance calculated for the bulk, 2.126 Å, to be compared with the experimental distance of 2.104 Å[30]). The atomic structure is optimized until all atomic forces are less than 0.01 eV/Å. Adsorbates and defects are situated on one side of the slab with 12 Å of vacuum separation to the nearest periodic image cell; there is 1 adsorbate for each 32 surface atoms, corresponding to a coverage $\theta = 0.03$. Detailed tests have shown that a sampling of the Brillouin zone using a $(2 \times 2 \times 1)$ k-point mesh resulted in a converged total energy. We have performed spin-polarized calculations for all systems to check the stability of triplet versus singlet states.

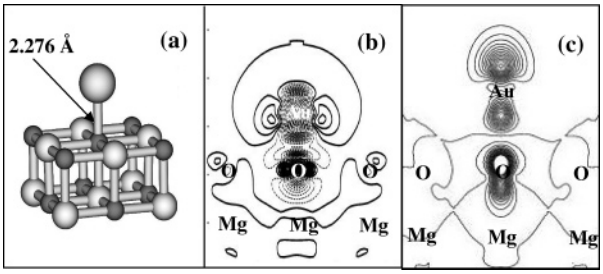

Figure 1. (a) Structure of a Au atom adsorbed on a five-coordinated oxygen ion, O_{5c}, on the MgO(100) terrace (white atoms, Mg; black atoms, O; large gray atoms, Au). (b) Charge density difference for Au_1/MgO O_{5c} (solid lines, charge accumulation; dotted lines, charge depletion). (c) Spin density for Au_1/MgO O_{5c}. Lines are drawn in intervals of 0.01 e/Å^3.

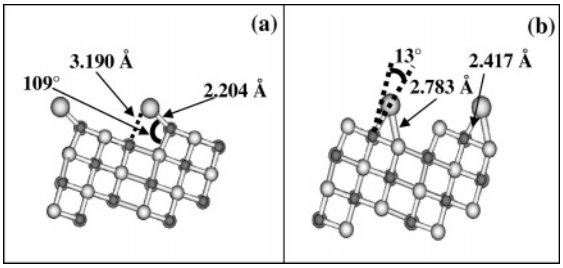

Figure 2. Structure of a Au atom adsorbed on a four-coordinated oxygen ion, O_{4c}, on a MgO step (white atoms, Mg; black atoms, O; large gray atoms, Au): (a) lowest isomer; (b) local minimum on a five-coordinated oxygen on the terrace.

The theoretical description of the paramagnetic F_s^+ center requires some comment (the s subscript indicates that the defect is on the surface). Formally, the F_s^+ center is obtained by removing an O^- ion from the surface, thus leaving behind a paramagnetic defect with a net positive charge.[31] For this reason this center cannot be treated in a simple way in a periodic approach. However, neutral models of oxygen vacancies with one trapped electron can be obtained in periodic calculations by doping the surface with H[32] or Na[33] atoms. Here we adopted this procedure, and we replaced the Mg atom at the bottom of the vacancy with a Na atom, thus introducing an impurity level in the gap. The unpaired electron is localized in the center of the vacancy,[34] and the defect has properties similar (not identical) to those of the classical F_s^+ defect;[31,32] notice that the whole system is neutral, at variance with the "real" F_s^+ center. Still, we will use the notation "F_s^+ center" to indicate this paramagnetic oxygen vacancy. Recent embedded cluster and periodic supercell calculations have shown that most of the properties of a charged F_s^+ center are correctly reproduced by the model of Na-doped MgO with an oxygen vacancy.[34]

3. Results

3.1. Au Atoms. The high ionization potential of gold ($IP_{exp} = 9.2$ eV,[35] $IP_{theory} = 9.58$ eV) disfavors charge transfer processes from Au to the surface; in principle, an electron attachment to Au is more likely given the relatively high electron affinity of the atom ($AE_{exp} = 2.3$ eV,[35] $AE_{theory} = 2.31$ eV). We will see below that in fact there is little charge transfer between Au and regular sites of MgO. We have considered different adsorption sites (Table 1): the ideal flat terrace, an oxygen vacancy on a terrace (F_s or F_s^+ center, depending on the number of electrons associated with the cavity, one, F_s^+, or two, F_s), a Mg−O divacancy at a terrace, and a monatomic step.

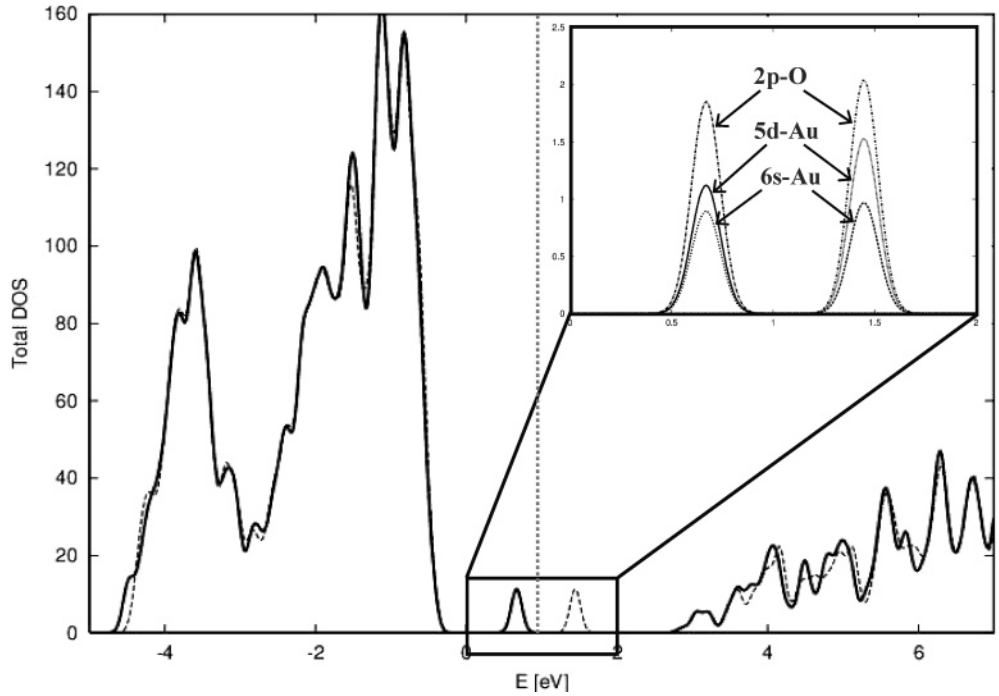

Figure 3. Density of states for a Au atom adsorbed on a five-coordinated oxygen ion, O_{5c}, on the MgO(100) terrace (solid line, α spin; dotted line, β spin). In the inset are shown the projected DOSs onto the Au 6s, 5d, and O 2p states in the energy range 0−2 eV.

We define the adsorption energy of the gold adatom or cluster, E_a, at a specific site as

$$E_a = -E(\mathrm{Au}_n/\mathrm{MgO\ site}) + E(\mathrm{Au}_n) + E(\mathrm{MgO\ site}) \quad (1)$$

With this convention, a positive value means an attractive interaction. Transition-metal atoms deposited on the MgO surface prefer to bind to the anion sites. On the flat terraces of MgO these are the five-coordinated oxide anions, O_{5c}. Au forms a bond of 0.89 eV with a Au−O_{5c} distance of 2.28 Å, Table 1 and Figure 1a. The binding energy is somewhat larger than other theoretical estimates previously reported,[21,22] but this is related to the tendency of the PW91 GGA functional to slightly overbind. Oxide anions are also present at steps, where the coordination is lower, O_{4c}. In the most stable adsorption site at a step the gold atom interacts with both the O_{4c} ion of the step, d(Au−O_{4c}) = 2.20 Å, and the O_{5c} ion of the lower plane, d(Au−O_{5c}) = 3.19 Å, Figure 2a. The binding energy, 1.26 eV, Table 1, is 40% higher than on the terrace site. There is another local minimum where the gold atom is sitting on an O_{5c} ion close to the step, Figure 2b: E_a for this configuration, 0.85 eV, is nearly the same as that obtained for a flat terrace, showing that the perturbation of the surface potential determined by a line defect such as a step is local and restricted to the low-coordinated atoms at the step.

To analyze the bonding mechanism, we have determined the charge density difference maps by subtracting from the charge density of the interacting system the densities of the separated units (substrate and adsorbate computed with the same super cell, geometry, etc.). The difference is positive (negative) in the regions where there is accumulation (depletion) of electronic charge. The map, Figure 1b, clearly shows that the changes in the charge density are restricted to the gold atom and to the oxygen ion where Au is adsorbed; the rest of the oxide remains unperturbed, indicating that the bond has a very local nature. Similar maps are obtained for a Au atom bound at a step and are not shown. The lack of accumulation of electron density in the region between Au and the surface suggests important bonding contributions from intraunit polarization. On the other hand, the fact that the spin density, Figure 1c, is partially delocalized over the O_{5c} ion indicates the existence of some covalent mixing.

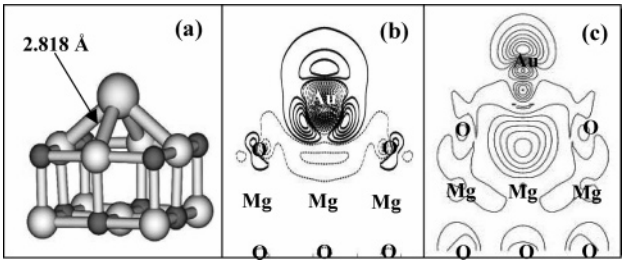

Figure 4. (a) Structure of a Au atom adsorbed on an oxygen vacancy, F_s, on the MgO(100) terrace (white atoms, Mg; black atoms, O; large gray atoms, Au). (b) Charge density difference for Au_1/MgO F_s (solid lines, charge accumulation; dotted lines, charge depletion). Lines are drawn in intervals of 0.007 e/Å^3. (c) Spin density map for Au_1/MgO F_s. Lines are drawn in intervals of 0.01 e/Å^3.

This conclusion is further supported by the analysis of the density of states (DOS) of the MgO(100) and MgO(100)/Au systems. All the DOS curves have been translated to allow the zero of the energy to coincide with the top of the O 2p valence band (defined by the highest O 2p states of the surface oxygen anions not directly interacting with the Au atom). The total DOS for the MgO(100)/Au system (shown in Figure 3 for a terrace, but very similar for a step) shows the presence of two isolated electronic states in the gap, one associated with the α-component of the Au 6s level (filled) and the other with the empty β-component. The 6s level is partially mixed with the Au 5d states and, to a larger extent, with the 2p levels of the oxide anion to which Au is bound. This confirms that besides the intraunit polarization, a contribution to the Au−MgO bond strength comes from a covalent mixing of the Au and O valence levels. The Au 6s level lies about 1 eV above the top of the MgO valence band, Figure 3. Since the gap for the MgO surface in DFT is underestimated (∼3.2 eV compared to 6.7 eV),[38] one can qualitatively rescale the position of the 6s level, which is

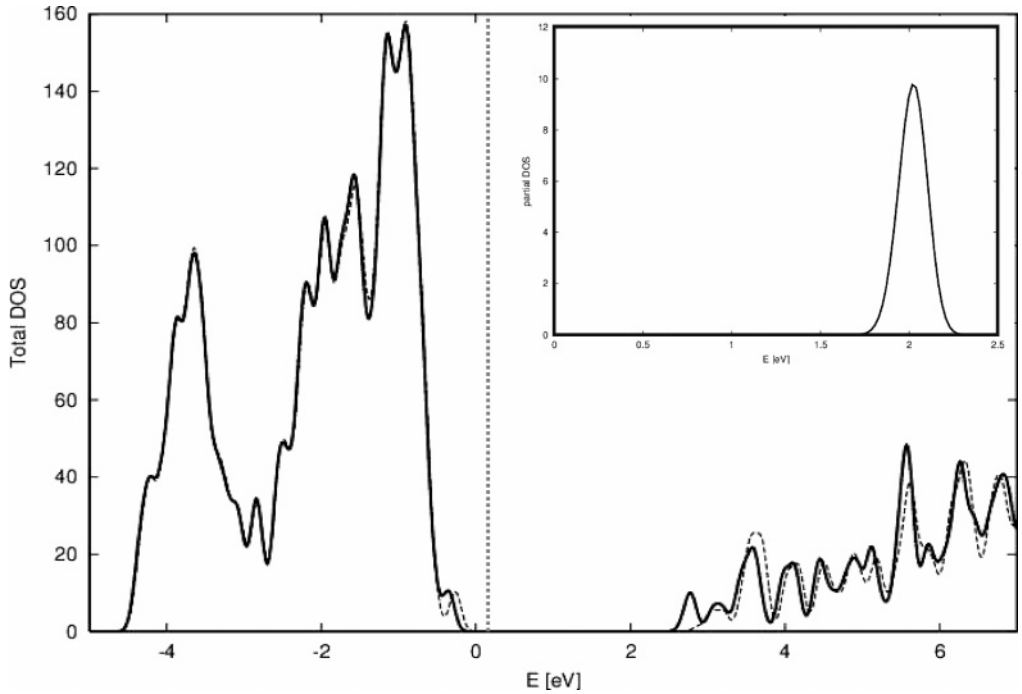

Figure 5. Density of states for a Au atom adsorbed on an oxygen vacancy, F_{5c}, on the MgO(100) terrace. In the inset are shown the total DOSs of the F_{5c} center without adsorbate in the energy range 0−2.5 eV. The peak in the inset around 2 eV is due to the electrons trapped in the F_{5c} center.

predicted to be about 2 eV above the top of the valence band. This is the same position of metal-related states observed in MIES experiments on Ag adsorption on MgO.[36]

It is known that the bonding of metal atoms on oxide surfaces becomes much stronger when it involves oxygen vacancies.[22,37] On an F_s center of MgO the vertical distance of Au from the surface is $z_{Au} = 1.791$ Å, Figure 4a, and the adsorption energy becomes 3.17 eV, i.e., almost 4 times larger than on the regular sites. The electron density inside the cavity is easily polarizable, and can even be transferred to the adsorbed atom, also considering the high EA of Au. This leads to the formation of a strong covalent polar bond, with partial charge transfer to the metal. This is clear from the plots of the spin and charge density maps, Figure 4b,c. They show an accumulation of charge in the region occupied by the Au atom, Figure 4c, due to a partial electron transfer from the vacancy. This is confirmed also by the plot of the spin density, Figure 4b: the spin is partially located in the cavity, indicating that the electron density has been removed from the vacancy and transferred to the 6s level of Au.

The total DOS for the bare F_s center, see the inset in Figure 5, shows a doubly occupied impurity state in the gap about 2.3 eV above the top of the O 2p valence band. This level is higher in energy than the 6s level of a Au atom bound to an O_{5c} ion, Figure 3. Thus, when Au is placed over an oxygen vacancy, the electronic charge flows from the F_s level to the 6s orbital of Au, which becomes formally negatively charged. The DOS of the MgO F_s/Au interacting system shows that the vacancy-related peak and the Au 6s level are pushed toward the O 2p band by the effect of the mutual interaction and contribute to form new states just above the top of the O 2p valence band, Figure 5.

We consider now the interaction of Au with the F_s^+ center, Figure 6a. We find a large adsorption energy, 3.97 eV, and a short distance, $z_{Au} = 1.56$ Å, due to the coupling of the unpaired electron in the vacancy with that of Au, with formation of a two-center, two-electron bond. Consistently, the charge density difference map, Figure 6b, shows an accumulation of charge

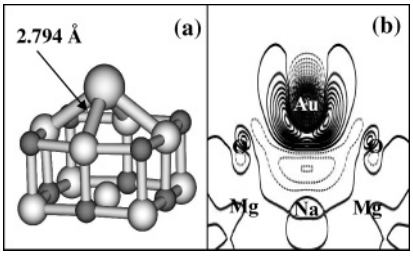

Figure 6. (a) Structure of a Au atom adsorbed on a paramagnetic oxygen vacancy, F_s^+, on the MgO(100) terrace (white atoms, Mg; black atoms, O; large gray atoms, Au). (b) Charge density difference for Au_1/MgO F_s^+ (solid lines, charge accumulation; dotted lines, charge depletion). Lines are drawn in intervals of 0.005 e/Å^3.

between the gold atom and the surface. An additional proof of the covalent character of this bond comes from the DOS curves. In Figure 7 we report the DOS of our model of an F_s^+ center. This is a spin-polarized system, and in fact, there are two peaks in the gap, one occupied and one empty. The position of these peaks with respect to the top of the valence band is similar to that of the neutral F_s center, while real F_s^+ centers generate impurity levels much closer to the top of the valence band because of the net charge associated with the defect.[38] This effect has to be taken into account in the discussion of the Au−F_s^+ bonding nature and in particular of the bond polarity. The DOSs of the MgO F_s^+/Au system (not shown) do not exhibit the presence of states in the gap: the electron in the vacancy is coupled with the 6s electron of Au, with partial charge transfer to the metal atom, consistent with the fact that the position of the 6s level is below that of the F_s^+ level. However, in our model the extent of charge transfer is partly exaggerated by the neutral state of the paramagnetic oxygen vacancy ("F_s^+").

The last site considered is the divacancy, a center formed by removing a Mg−O pair from the surface. Recent AFM experiments have pointed out the possible existence of these defects on UHV-cleaved MgO single-crystal surfaces;[39] it is also a site where nucleation of small metal clusters is preferred.[10,15] Among the several positions on a divacancy where the Au atom

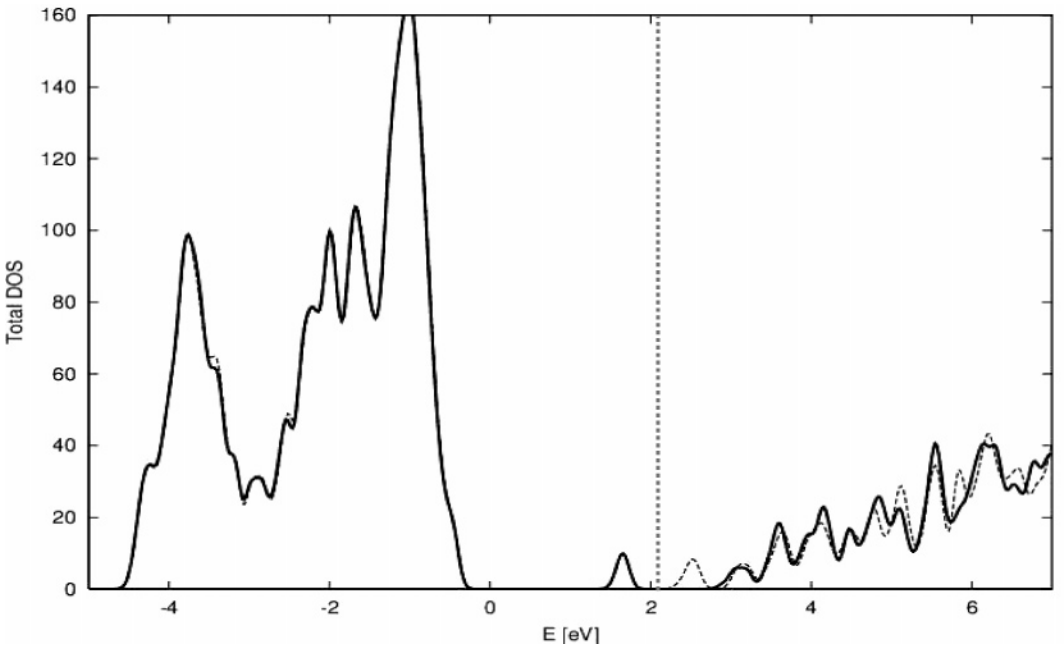

Figure 7. Density of states for a paramagnetic oxygen vacancy, F_s^+, on the MgO(100) terrace (solid line, α spin; dotted line, β spin). Notice that the calculation has been performed within a supercell approach by doping the MgO slab with a Na atom, thus introducing a single electron in the oxygen vacancy. In this respect the reported DOS refers to a neutral center, and the notation "F_s^+" is only meant to indicate the paramagnetic nature of the defect center.

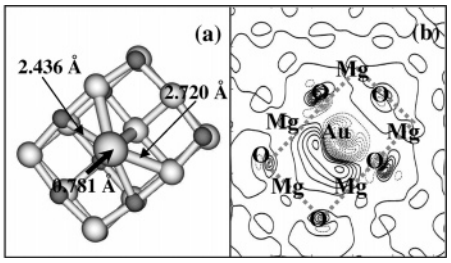

Figure 8. (a) Structure of a Au atom adsorbed on an oxygen divacancy on the MgO(100) terrace. (b) Charge density difference for Au_1/MgO divacancy (solid lines, charge accumulation; dotted lines, charge depletion). Lines are drawn in intervals of 0.01 e/Å^3.

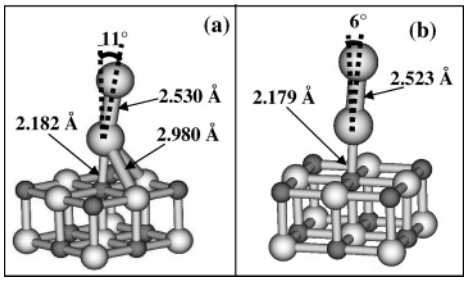

Figure 9. Structure of the two lowest isomers for Au_2 adsorbed on a five-coordinated oxygen ion, O_{5c}, on the MgO(100) terrace (white atoms, Mg; black atoms, O; large gray atoms, Au): (a) Au_2 tilted toward an oxygen atom; (b) Au_2 tilted toward a magnesium atom.

can be stabilized, the most stable one (E_a = 2.36 eV, Table 1) corresponds to the Au atom adsorbed in the position of the missing Mg atom, Figure 8a. Au can also sit on the oxygen anion at the border of the divacancy; in this case we find two minima with smaller adsorption energies, around 1.10 eV. Looking at the charge density difference maps, Figure 8b, we see that the bond between Au and the divacancy has strong polar character. The large binding energy is due to the strong field created by the removal of the Mg−O pair from the surface (for a detailed discussion of the electronic structure of a divacancy see refs 40 and 41).

3.2. Au Dimers. Gas-phase Au_2 has a $^1\Sigma_g$ ground state, with a D_e of 2.30 eV and an equilibrium distance of 2.520 Å, considerably shorter than in bulk gold, 2.88 Å.[35] The computed values are D_e = 2.32 eV and r_e = 2.47 Å, and the agreement with the experimental values provides an indication of the quality of the calculations. In the triplet excited state, Au_2 is bound by only 0.50 eV and the Au−Au distance becomes 2.76 Å. When the dimer is supported on the MgO surface, the ground state remains singlet, irrespective of the adsorption site.

We define some key quantities to analyze the tendency of adsorbed Au atoms to nucleate and form nanoclusters.[10] The adsorption energy of the dimer, E_a, has been defined in eq 1 and measures the strength of the interaction of the Au_2 molecule with the substrate. Besides E_a we define two other energies:

$$E_{\mathrm{dim}} = -E(\mathrm{Au}_n/\mathrm{MgO\ site}) + E(\mathrm{Au}) + E(\mathrm{Au}_{n-1}/\mathrm{MgO\ site})\ (n = 2) \quad (2)$$

$$E_{\mathrm{b}} = -E(\mathrm{Au}_n/\mathrm{MgO\ site}) - E(\mathrm{MgO\ terrace}) + E(\mathrm{Au}_{n-1}/\mathrm{MgO\ site}) + E(\mathrm{Au}_1/\mathrm{MgO\ terrace}) \quad (3)$$

E_{dim} is the binding energy of a gas-phase Au atom to a Au atom already bound to a given site, and E_b is the dimer surface formation energy, a quantity which measures the stability of the adsorbed dimer with respect to two gold adatoms, one bound at a given site (e.g., a defect) and the other on a terrace O_{5c} anion. E_b is an important quantity in constructing kinetic models of the growth of metal clusters on oxide surfaces. Metal atoms are deposited from the gas phase to the surface, where they diffuse rapidly until they are trapped at a strong binding site (typically a defect). Metal atoms diffusing on the surface have a given probability to collide with a trapped adatom. If the energy gained in the formation of the dimer exceeds the binding energy of the atom to a regular terrace site, a stable dimer can form. E_b provides a measure of the thermodynamic stability and of the tendency of adsorbed adatoms to dimerize.

On the MgO(100) flat terrace there are two geometries for the adsorbed dimer which are practically isoenergetic: in both

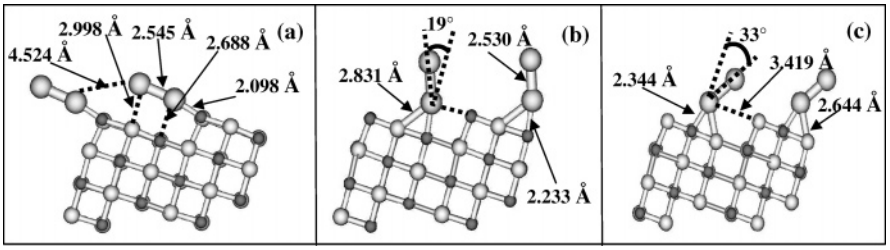

Figure 10. Structure of the three lowest isomers for Au_2 adsorbed on a four-coordinated oxygen ion, O_{4c}, on a MgO step (white atoms, Mg; black atoms, O; large gray atoms, Au).

of them, one Au atom is adsorbed on an O_{5c} anion and the molecular axis is slightly tilted with respect to the surface normal, either toward the nearest Mg cation or toward the nearest O anion, Figure 9. The Au−Au distance in the two configurations is 2.52−2.53 Å, i.e., practically unchanged with respect to that of the free molecule. Au_2 is bound to the surface by 1.49 eV, Table 1, 0.6 eV more than a single Au atom because of the higher polarizability of the dimer. The energy difference between the two configurations is only 0.01 eV, indicating free rotation and flipping around the equilibrium position. The normal orientation is about 0.3 eV higher than the two tilted configurations and represents a saddle point connecting the two minima. E_b is almost 2 eV, indicating a large energy gain of the dimerization; however, this value is very close to the dissociation energy of gas-phase Au_2, 2.32 eV, showing that the perturbation of the regular MgO sites on the Au−Au bond is very small.

On a monatomic step on the MgO surface the most stable configuration for the dimer is with one Au atom interacting simultaneously with the O_{4c} ion of the step and with the O_{5c} ion of the lower plane, and the second Au atom almost above a Mg ion of the lower plane, Figure 10a. The molecule lies almost parallel to the surface, and the Au−Au distance, 2.545 Å, is slightly elongated compared to that of gas-phase Au_2. This configuration is only 0.05 eV more stable than an isomer where the dimer is slightly tilted toward an oxygen anion of the lower terrace (not shown). The preference for the symmetric configuration could be influenced by the size of the supercell used for the calculations, and the resulting weak adsorbate−adsorbate interactions. Two other structures correspond to local minima and are about 0.5 eV higher in energy. They differ from the lowest isomer in the fact that the Au−Au axis is almost normal to the (100) planes, Figure 10b,c. These two adsorption modes are reminiscent of a gold dimer adsorbed on a (100) terrace, with the difference that they are in the vicinity of a step. Thus, it is not surprising that the adsorption properties and in particular the adsorption energy are close to those found for the Au dimer on a flat terrace.

E_b for the most stable isomer formed on a step, 2.23 eV, is only 0.24 eV higher than on the terrace, Table 1. Thus, while the adsorption energy of the dimer on the step is 0.58 eV higher than on a terrace, E_b is only 10% higher, suggesting the monoatomic steps are not markedly preferential nucleation sites compared to flat terraces (at least not from a thermodynamic point of view).

On an F_s center the dimer exhibits various geometries corresponding to local minima. In the lowest structure the Au_2 molecule is tilted by 57° toward a Mg ion at the border of the defect, Figure 11a; E_a for the whole cluster is 4.17 eV. This means that clusters formed on oxygen vacancies will not diffuse as a whole but rather add or lose metal atoms, thus changing their size. Another minimum for Au_2 on F_s, slightly higher in energy, $E_a = 3.91$ eV, is found when the tilt of the molecule is

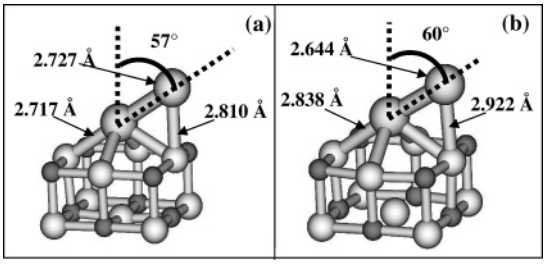

Figure 11. (a) Structure of the lowest isomers for Au_2 adsorbed on an oxygen vacancy, F_s, on the MgO(100) terrace and (b) structure of the lowest isomers for Au_2 adsorbed on a paramagnetic oxygen vacancy, F_s^+, on the MgO(100) terrace (white atoms, Mg; black atoms, O; large gray atoms, Au).

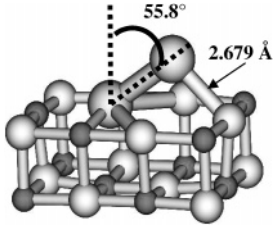

Figure 12. Structure of the lowest isomers for Au_2 adsorbed on a divacancy on the MgO(100) terrace (white atoms, Mg; black atoms, O; large gray atoms, Au).

toward the oxygen ion of the border. The structure corresponding to the dimer normal to the surface is also a minimum, almost isoenergetic with the second one ($E_a = 3.89$ eV). These results are in agreement with those reported by Bogicevic and Jennison,[17] who found the same absolute minimum and a similar energetics. The dimer binding energy on the F_s center, E_b, is 2.42 eV, and shows a further increase with respect to that of the step.

Also on an F_s^+ center the structure of the dimer is tilted toward the Mg cation at the border of the vacancy, Figure 11b. The geometry is very similar to that found on the neutral F_s center, but the energetics is quite different. The dimer is strongly bound to the surface, $E_a = 2.82$ eV, but the gain to form the dimer from two gold atoms, one sitting on the F_s^+ center and the other one on the MgO terrace, is very small, $E_b = 0.26$ eV, Table 1. This is a consequence of having one unpaired electron in the vacancy which is coupled with the 6s electron of the Au atom, forming a two-electron, two-center F_s^+−Au bond. When the second atom is added to this closed shell system, the interaction is weak and entirely due to polarization effects. Thus, F_s^+ centers and in general paramagnetic defects are not good nucleation sites for Au on MgO.

Finally, we consider a dimer formed at a divacancy. One of the two gold atoms is adsorbed in the divacancy, close to the lattice position previously occupied by a Mg cation; the molecular axis is tilted by 56° with respect to the surface normal, Figure 12. For this defect no other minima have been found,

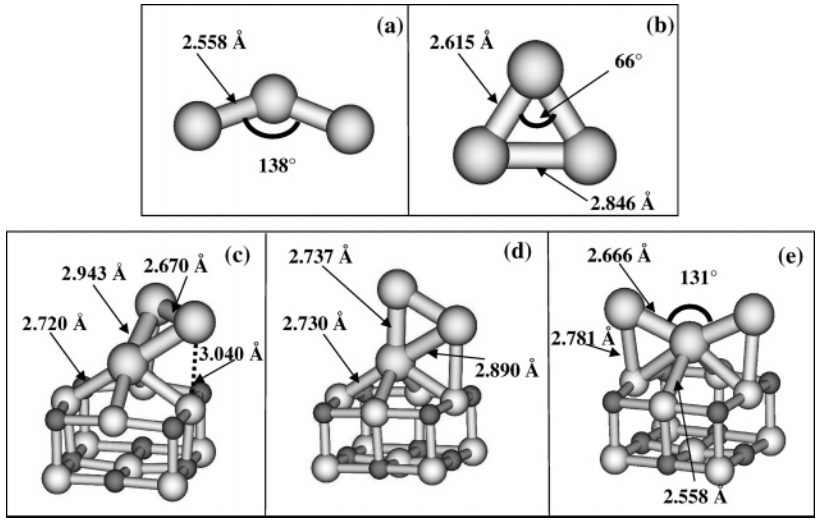

Figure 13. (a, b) Structure of gas-phase isomers of Au_3 and (c−e) structure of the three lowest isomers for Au_3 adsorbed on an oxygen vacancy, F_s, on the MgO(100) terrace (white atoms, Mg; black atoms, O; large gray atoms, Au).

despite specific attempts to locate them. The dimer binds quite strongly to the divacancy, $E_a = 2.97$ eV, i.e., almost twice the value found for Au_2 on a regular terrace site, Table 1. Despite this strong adhesion to the surface, E_b for a divacancy is 2.06 eV, only 0.07 eV higher than on a terrace and less than on a step or on an F_s center.

In all the cases discussed, with the exception of the F_s^+ center, the energy gain associated with the dimerization of two Au adatoms is about 2 eV, similar to the Au−Au bond strength in the gas phase. On an F_s^+ center the gain is only 0.26 eV, but this is connected to the open shell nature of this center. The fact that the dimer binding energy is nearly the same on all other sites considered means that the MgO defects are not too important in the phase of dimer formation while they are crucial in the step of trapping the diffusing metal atoms (or clusters) and reduce the atomic mobility on the surface. When looking at these sites in detail, however, the most favorable one for dimer formation is the F_s center.

To better understand the growing mechanism, we have estimated the diffusion energy of gold atoms on the (100) surface. We have considered the two most likely diffusion paths on a flat terrace: in path 1, O−O, the metal moves directly from one oxide anion to the nearest neighbor oxygen through the diagonal of the square lattice; in path 2, O−Mg−O, the atom diffuses from one oxygen atom to the nearest Mg cation and then to oxygen. The energy associated with path 1 is 0.24 eV only, while path 2 has a barrier of about 0.6 eV. One should mention that these are not real barriers as we did not try to locate the transition state in the diffusion process. The values have been obtained by optimizing the vertical distance of the Au atom from the center of the O−O bond or from the Mg cation. Nevertheless, the reported values provide a good estimate of the energy involved in the diffusion process. The low barrier for diffusion, 0.24 eV, indicates that the atoms are mobile even at low temperatures. At 100 K, using the calculated diffusion barrier, $E_d = 0.24$ eV, and an Arrhenius expression from transition-state theory,[42] a hopping frequency of ∼7.5 Hz and a resident time 0.1 s are computed, indicating limited mobility of the adsorbed atoms. Already at 200 K the mobility becomes extremely high: a hopping frequency of ∼8.7 MHz and a resident time of 10^{-7} s. With respect to dimer formation, the calculations show that two Au atoms adsorbed on neighboring O^{2-} ions on the terrace spontaneously form the dimer in a nonactivated process.

TABLE 2. Properties of Free Au_3 and Au_3 Supported on a Neutral Oxygen Vacancy on the MgO Surface

	gas phase		F_s center		
	Figure 13a	Figure 13b	Figure 13c	Figure 13d	Figure 13e
E_a,[a] eV			4.55	4.47	4.35
E_{trim},[b] eV	1.33	1.24	1.81	1.73	1.61
E_b,[c] eV			0.99	0.91	0.69
r(Au−S), Å			2.72	2.73	2.56
r(Au−Au), Å	2.56	2.62, 2.85	2.67, 2.94	2.74, 2.89	2.67

[a] $E_a = -E(Au_3/MgO\ F_s) + E(Au_3) + E(MgO\ F_s)$. [b] $E_{trim} = -E(Au_3/MgO\ F_s) + E(Au) + E(Au_2/MgO\ F_s)$ for supported Au_3 or $E_{trim} = -E(Au_3) + E(Au) + E(Au_2)$ for gas-phase Au_3. [c] $E_b = -E(Au_3/MgO\ F_s) - E(MgO\ O_{5c}) + E(Au_2/MgO\ F_s) + E(Au_1/MgO\ O_{5c})$.

3.3. Au Trimers. In this section we consider the formation of a Au_3 nanocluster on the MgO surface. We have seen in the previous section that the dimerization process is not particularly affected by the adsorption site (at variance with Pd, where this has strong influence on the nucleation).[10] This is largely due to the coupling of the 6s electrons of the two Au atoms, a process which is not significantly affected by the site where the atoms are bound (except for paramagnetic defects such as, for instance, the F_s^+ center). On this basis, it is likely that the formation of a trimer, $Au_2(ads) + Au(ads) \rightarrow Au_3(ads)$, becomes the critical step in the nucleation process. In fact, the trimerization implies the addition of a ^2S atom to a closed shell dimer. The process has been considered on the F_s center only, a prototype of point defects at the MgO surface and a site where Au atoms have a high trapping energy. The study has preliminary character, and we plan to extend it to other sites in the future.

The Au_3 molecule in the gas phase has a doublet ground state. We find that in the most stable geometry the three atoms form an angle of 138°, Figure 13a, but another structure with an internal angle of 66°, Figure 13b, is only slightly higher in energy (∼0.1 eV), suggesting a fluxional behavior of the molecule at finite temperatures. The bent shape predicted by our calculations is in agreement with the GGA results of Häkkinen et al.,[43] while Wang et al.,[44] using an LDA approach, found a linear structure for the lowest isomer. The formation of Au_3 in the gas phase from $Au_2 + Au$ is accompanied by an energy gain of 1.33 eV, Table 2.

We have applied to this system the same energy analysis used for the dimers adsorbed on the MgO surface; see eq 3 and Table 2. On an F_s center we located at least three energy minima for

Au_3, in an energy range of 0.1 eV; in two cases the Au atoms form an isosceles triangle, Figure 13c,d, while in the third one the Au atoms form a more open bent structure, Figure 13e. We cannot exclude that other isomers with similar energies exist. This suggests a fluxional behavior also when the cluster is bound to an oxygen vacancy, despite the strong interaction, E_a = 4.55 eV, typical of adsorption on F_s centers. This may have important consequences for the reactivity of supported Au clusters toward gas-phase molecules. The addition of a Au atom to the dimer leads to an energy gain, E_b = 0.99 eV, Table 2, sufficiently high to guarantee that, once formed, the trimer will stay intact for sufficiently long times. Thus, F_s centers are excellent sites for nucleation of Au clusters since they trap isolated atoms, favor the addition of a second atom with formation of the dimer, and finally allow the addition of a third atom, starting the growth of a metal cluster.

4. Conclusions

We have considered the adsorption of Au atoms and dimers on various sites of the MgO surface (terraces, steps), including defects such as single and double vacancies. On MgO terraces or steps Au prefers to bind to the oxide anions with a bond which has partial covalent and partial polarization contributions. The fact that the spin density is not exclusively localized on Au but involves also the 2p orbitals of the oxide anion to which Au is bound shows a significant degree of orbital mixing. The covalent contribution to the metal−oxide bonding is largest for F_s and F_s^+ centers, with considerable charge transfer from the defect to the Au atom (in particular for F_s centers). This is a consequence of the large electron affinity of Au, 2.3 eV, and explains why under some circumstances one can assist the formation of stable supported Au^- species on MgO.[45] On an F_s^+ center the bonding arises mainly from the direct coupling of the unpaired electron of the vacancy with the 6s electron of Au. The last case considered is that of a divacancy, where the metal atom can interact with two low-coordinated oxygen ions, giving rise to a substantial interaction energy.

The energy gain connected to the formation of the dimer by aggregation of two diffusing atoms is similar, $E_b \approx 2$ eV, for all sites considered with the exception of the paramagnetic F_s^+ center. This is because the spin coupling (formation of a direct Au−Au bond) leads to a net stabilization which is not very affected by the strength of the Au−surface bond. On an F_s^+ center the formation of a strong covalent bond between the surface and the Au atom results in a low tendency of the surface complex to add additional Au atoms. In this respect, paramagnetic defects on the MgO surface are not good dimerization centers for metals such as Cu, Ag, or Au.

Since Au atoms diffuse almost freely on the surface (the estimated diffusion barrier is about 0.2 eV), the critical step for cluster nucleation is the capture of these atoms by strong trapping sites. Among all considered sites, the F_s and F_s^+ centers are clearly the most efficient trapping sites. Only the F_s defect is then a good site for dimer formation, appearing as an excellent candidate for the nucleation of Au clusters. In addition, there is a finite probability that Au dimers and small clusters form on terrace sites and then diffuse until they remain trapped on a defect. The density of defects is $\sim 10^{12}$ cm^{-2} on MgO thin films, while on UHV-cleaved MgO single crystals it is between 10^{11} and 10^{13} cm^{-2}. This is also the Au cluster density on MgO.[20] The role of the point defects in anchoring the clusters is shown by recent AFM experiments which have demonstrated that the cluster density remains nearly constant with the deposition time,[20] indicating that a higher flux of Au atoms results in larger clusters and not in a higher density of clusters.

These results show that substantial differences exist in the mechanism of nucleation and growth of Pd and Au clusters on the MgO surface. For Pd, which has a closed shell atomic ground state, the metal−oxide interaction prevails over the metal−metal one, and the dimerization process has different energetics from site to site;[10] for Au, which has an open shell ground-state structure, the metal−metal interaction prevails over the metal−oxide one, and the dimerization is a favorable process on a large choice of the adsorption sites.

Acknowledgment. This work has been supported by the European Union through the FP6 STRP project GSOMEN, by the Italian Ministry of University and Research (MIUR) through a Cofin 2003 project, and by the Italian INFM through the initiative "Calcolo Parallelo". A.D.V. thanks the Marie Curie program for financial support of her visit to the Ecole Normale Superieure de Lyon.

References and Notes

(1) Freund, H.-J. *Surf. Sci.* **2002**, *500*, 271.
(2) Haruta, H. *Catal. Today* **1997**, *36*, 153.
(3) Chen, M. S.; Goodman, D. W. *Science* **2004**, *306*, 252.
(4) Sanchez, A.; Abbet, S.; Heiz, U.; Schneider, W. D.; Ferrari, A. M.; Pacchioni, G.; Rösch, N. *J. Am. Chem. Soc.* **2000**, *122*, 3453.
(5) Sanchez, A.; Abbet, S.; Heiz, U.; Schneider, W. D.; Häkkinen, H.; Barnett, R. N.; Landmann, U. *J. Phys. Chem. A* **1999**, *103*, 9573.
(6) Bäumer, M.; Freund, H. J. *Prog. Surf. Sci.* **1999**, *61*, 127.
(7) Rodriguez, J. A.; Perez, M.; Jirsak, T.; Evans, J.; Hrbek, J.; Gonzales, L. *Chem. Phys. Lett.* **2004**, *378*, 526.
(8) Häkkinen, H.; Abbet, S.; Sanchez, A.; Heiz, U.; Landman, U. *Angew. Chem., Int. Ed.* **2003**, *42*, 1297.
(9) Haas, G.; Menck, A.; Brune, H.; Barth, J. V.; Venables, J. A.; Kern, K. *Phys. Rev. B* **2000**, *61*, 11105.
(10) Giordano, L.; Di Valentin, C.; Goniakowski, J.; Pacchioni, G. *Phys. Rev. Lett.* **2004**, *92*, 096105.
(11) Pacchioni, G. *ChemPhysChem* **2003**, *4*, 1041.
(12) Abbet, S.; Riedo, E.; Brune, H.; Heiz, U.; Ferrari, A. M.; Giordano, L.; Pacchioni, G. *J. Am. Chem. Soc.* **2001**, *123*, 6172.
(13) Judai, K.; Abbet, S.; Wörz, A. S.; Heiz, U.; Giordano, L.; Pacchioni, G. *J. Phys. Chem. B* **2003**, *107*, 9377.
(14) Giordano, L.; Del Vitto, A.; Pacchioni, G.; Ferrari, A. M. *Surf. Sci.* **2003**, *540*, 63.
(15) Bogicevic, A.; Jennison, D. R. *Surf. Sci.* **1999**, *437*, L741.
(16) Yang, Z.; Wu, R.; Zhang, Q.; Goodman, D. W. *Phys. Rev. B* **2002**, *65*, 155407.
(17) Bogicevic, A.; Jennison, D. R. *Surf. Sci.* **2002**, *515*, L481.
(18) Guzman, J.; Gates, B. C. *Nano Lett.* **2001**, *1*, 689.
(19) Molina, L. M.; Hammer, B. *Phys. Rev. B* **2004**, *69*, 155424.
(20) Højrup-Hansen, K.; Ferrero, S.; Henry, C. R. *Appl. Surf. Sci.* **2004**, *226*, 167.
(21) Yudanov, I.; Pacchioni, G.; Neyman, K.; Rösch, N. *J. Phys. Chem.* **1997**, *101*, 2786.
(22) Matveev, A. V.; Neyman, K.; Yudanov, I.; Rösch, N. *Surf. Sci.* **1999**, *426*, 123.
(23) Kubo, M.; Miura, R.; Yamauchi, R.; Vetrivel, R.; Miyamoto, A. *Appl. Surf. Sci.* **1995**, *89*, 131.
(24) Hohenberg, P.; Khon, W. *Phys. Rev.* **1964**, *136*, B864.
(25) Kohn, W.; Sham, L. J. *Phys. Rev.* **1965**, *140*, A1133.
(26) Kresse, G.; Hafner, J. *Phys. Rev. B* **1993**, *47*, 558. Kresse, G.; Fürthmuller, J. *Phys. Rev. B* **1996**, *54*, 11169.
(27) Blöchl, P. E. *Phys. Rev. B* **1994**, *50*, 17953.
(28) Perdew, J. P.; Chevary, J. A.; Vosko, S. H.; Jackson, K. A.; Pederson, M. R.; Singh, D. J.; Fiolhais, C. *Phys. Rev. B* **1992**, *46*, 6671.
(29) Schinkte, S.; Messerli, S.; Pivetta, M.; Patthey, F.; Libioulle, L.; Stengel, M.; De Vita, A.; Schneider, W.-.D. *Phys. Rev. Lett.* **2001**, *87*, 276801.
(30) Wyckoff, R. W. G. *Crystal Structures*, 2nd ed.; Interscience: New York, 1965.
(31) Ferrari, A. M.; Pacchioni, G. *J. Phys. Chem.* **1995**, *99*, 17010.
(32) Ménétrey, M.; Markovits, A.; Minot, C.; Del Vitto, A.; Pacchioni, G. *Surf. Sci.* **2004**, *549*, 294.
(33) Hammer, B. Personal communication.
(34) Del Vitto, A.; Giordano, L.; Pacchioni, G.; Heiz, U. *J. Phys. Chem. B*, in press.
(35) *CRC Handbook of Chemistry and Physics*, 55th ed.; Weast, R. C., Ed.; CRC Press: Cleveland, OH, 1974.
(36) Stracke, P.; Krischok, S.; Kempter, V. *Surf. Sci.* **2001**, *473*, 86.

(37) Ferrari, A. M.; Pacchioni, G. *J. Phys. Chem.* **1996**, *100*, 9032.
(38) Shusko, P. V.; Shluger, A. L.; Catlow, C. R. A. *Surf. Sci.* **2000**, *450*, 153.
(39) Barth, C.; Henry, C. R. *Phys. Rev. Lett.* **2003**, *91*, 196102.
(40) Ojamäe, L.; Pisani, C. *J. Chem. Phys.* **1998**, *109*, 10984.
(41) Ricci, D.; Pacchioni, G.; Sushko, P. V.; Shluger, A. L. *J. Chem. Phys.* **2002,** *117*, 2844.
(42) Musolino, V.; Selloni, A.; Car, R. *J. Chem. Phys.* **1998**, *108*, 5044.
(43) Häkkinen, H.; Barnett, R. N.; Landmann, U. *Phys. Rev. B* **2000**, *62*, R2287.
(44) Wang, J.; Wang, G.; Zhao, J. *Phys. Rev. B* **2002**, *66*, 035418.
(45) Baistrocchi, M.; Giordano, L.; Del Vitto, A.; Pacchioni, G. To be published.